The Astrophysical Journal, 896:130 (9pp), 2020 June 20 https://doi.org/10.3847/1538-4357/ab8fb1

Polycyclic Aromatic Hydrocarbons as a Source for CH_N^+ ($N = 4$–6) and C_3H_2 in the Interstellar Medium

Roby Chacko, Shreyak Banhatti, Saroj Barik, and G. Aravind
Indian Institute of Technology Madras, Chennai 600 036, India; garavind@iitm.ac.in
Received 2020 March 10; revised 2020 April 23; accepted 2020 May 1; published 2020 June 19

Abstract

Photoionization and dissociation of anthracene, phenanthrene, and pentacene in the multiphoton regime at 266 nm wavelength were performed. CH_n^+ (n = 4–6) ions were observed as fragments, and their yields as a function of laser intensity were studied. H-migration and "roaming" mechanisms leading to the formation of these fluxional ions from polycyclic aromatic hydrocarbons (PAHs) are proposed. The present results show higher photostability of PAHs with bent structure and suggest PAHs in the UV regions of interstellar medium as a prominent source for CH_n^+ (n = 4–6).

Unified Astronomy Thesaurus concepts: Photodissociation regions (1223); Photoionization (2060); Polycyclic aromatic hydrocarbons (1280); Interstellar clouds (834); Dense interstellar clouds (371)

1. Introduction

Formation of single carbon cations such as CH_5^+ and CH_6^+, which are fluxional cations without any definite structure (McCoy et al. 2004; Wörner et al. 2007; Gerlich & Borodi 2009), have gained importance due to their role in astrochemistry (Asvany et al. 2004a, 2004b; Gerlich 2005; Gerlich & Smith 2006; Mann et al. 2008). Polycyclic aromatic hydrocarbons (PAHs) are proposed constituents of the interstellar medium (ISM), accounting for the observed emission in the 3–20 μm of the diffused interstellar bands (Allamandola et al. 1987; Salama et al. 1996, 1999; Peeters 2011). Recent investigations on the lifetimes of the XUV excited states of small PAHs strengthened their proposed presence in the ISM (Marciniak et al. 2015). UV Photodestruction of PAHs has been recently proposed as a pathway for formation of small hydrocarbons such as C_2H, c–C_3H_2, and C_4H based on their observed abundance in the photon-dominated or photodissociation regions (PDRs) in ISM (Fossé et al. 2000; Fuente et al. 2003; Teyssier et al. 2004; Pety et al. 2005). Moreover, studies on PAHs indicate the critical role of photodissociation in determining their lifetimes in the ISM. It is thus important to probe the photodestruction of PAHs as sources of these fluxional ions as well as other small hydrocarbons in the ISM.

CH^+ is one of the first molecules detected in the ISM (Douglas & Herzberg 1941; Cernicharo et al. 1997). CH_2^+ and CH_3^+ have been detected in the coma of comet Halley (Balsiger et al. 1987). The lack of intense lines in the (sub)millimeter range due to the absence of dipole moment renders the detection CH_3^+ and CH_4^+ ions formidable. Roueff et al. (2013) had searched for CH_2D^+ as an indirect search for CH_3^+ and detected the same.

Hydrocarbon cations with H/C ratios higher than one, such as CH_4^+, CH_5^+, CH_6^+, $C_2H_3^+$ and $C_2H_5^+$, cannot form via direct photodissociation of PAH molecules. These ions were observed in multiphoton ionization experiments on PAH molecules like naphthalene and tetracene (Robson et al. 2002; Poveda et al. 2008, 2009, 2010). Intramolecular hydrogen transposition or proton migration initiated by photofragmentation could lead to the formation of the highly protonated fragment ions (Poveda et al. 2009, 2010, 2013). An intense laser field could induce scrambling and intramolecular H-migration processes, paving the way to large-scale chemical bond rearrangement processes (Mineo et al. 2013; Kling et al. 2019; Wu et al. 2019). The H-atoms can change their location on a subnanosecond timescale (Gerlich & Borodi 2009). Kling et al. 2019 report the occurrence of single and double hydrogen migration processes in ethanal cations and dications that take place in a timescale of a few hundred femtoseconds to picoseconds. The exact pathway for the formation of the fluxional ions via photodissociation/ionization is yet to be understood, and our present results are of paramount importance in understanding the same, particularly in the ISM environment.

Apart from photoprocesses, formation of CH_5^+ and CH_6^+ are mainly perceived to be via protonation of CH_4, and H_2 addition to CH_3^+ and CH_4^+ (Gerlich & Horning 1992; Gerlich 2005; Gerlich & Smith 2006; Mann et al. 2008; Poveda et al. 2012b). Asvany et al. (2004a) propose the formation of CH_5^+ via an intermediary complex CH_6^+. CH_6^+ is a hypercoordinated carbocation with a short lifetime, which in turn is formed by the addition of H_2 to CH_4^+. For the formation of CH_5^+ and CH_6^+ in intense laser field, we suggest the possible interplay of the roaming mechanism, which is an alternative to the transition-state pathway in unimolecular decompositions (Townsend et al. 2004; Suits 2008; Bowman & Suits 2011). This mechanism was recently found in photodissociation dynamics (Lin et al. 2018) and its experimental and theoretical studies have gained momentum (Bowman & Houston 2017; Castellanos et al. 2018a, 2018b; Ekanayake et al. 2018a, 2018b; Wu et al. 2019; Iwamoto et al. 2020).

Since CH_n^+ (n = 4–6) play a vital role in astrochemistry and PAHs are proposed constituents of the ISM, in the current study we explore the formation of CH_n^+ (n = 4–6) via dissociative ionization of PAHs, namely, anthracene, phenanthrene, and pentacene. Anthracene and phenanthrene are isomers with linear and bent structures, respectively. The choice of these three PAHs is motivated by the aim to probe the dependence on the structure and size of the PAHs in the formation of CH_n^+ (n = 4–6), which form the main results of the present work. The physical and chemical conditions in PDRs are largely determined by the influence of far-ultraviolet

radiation (Hollenbach & Tielens 1997). Hence the 266 nm wavelength laser was chosen.

2. Experimental Results

A newly constructed experimental setup consisting of a Wiley–Mclaren time-of-flight (TOF; Wiley & McLaren 1955) with 80 cm long field-free drift region terminating with a multichannel plate detector was employed. Helium carrier gas seeded with vapors of precursor molecule (generated by heating) was injected into the first section of the acceleration region of the TOF using a pulsed valve. The fourth harmonic of Nd:YAG laser (266 nm) at 10 Hz repetition rate and 4 ns pulse duration was focused at the interaction region to a diameter of 6.3 μm using a lens of focal length 18.5 cm, yielding intensities at the order of 10^{13} W cm^{-2} at the focal point. The intensity was varied by changing the laser power. The experiments were carried out at laser powers ranging from 120 to 470 m Watts. The employed intensities correspond to a field strength of the order of 1–2 V Å^{-1}. The laser intensity (I) is calculated using the equation

$$I = \frac{\text{Energy per pulse / pulse duration}}{\text{focal area}} \quad (1)$$

and the field strength (E_0) is calculated using the equation

$$E_0 = \left(\frac{2I}{\epsilon_0 c}\right)^{1/2}, \quad (2)$$

where I is the intensity in W m^{-2}, ϵ_0 is the vacuum permittivity, and c is the speed of the light in vacuum. The base vacuum of the chamber was 10^{-8} mbar and was maintained below 10^{-5} mbar during the gas pulsing, providing a collisionless character of the molecular photofragmentation processes (Antonov & Letokhov 1981). The TOF data were collected using a FAST ComTec multihit data card (Model 7886). TOF data are typically accumulated for thousands of laser shots to see masses formed with meager yield.

Our results for the three molecules show extensive fragmentation than intact ionization, as shown in Figure 1. The extent of fragmentation with increasing laser intensities for the three molecules can be seen in Figure 2, particularly for masses less than 40 amu. A startling difference of phenanthrene spectra from its isomer anthracene or the larger molecule pentacene is the high yield of parent ion, despite the nanosecond laser pulsewidth.

Figure 3 shows the variation of fragment ion yield versus laser intensity for C^+, CH_n^+, and $C_2H_n^+$ fragments formed from anthracene and pentacene. The fractional values obtained for the slopes of the linear portion of each curve imply that the ionization/ dissociation process involves not only multiphoton processes but also field ionization as well.

The prominent fragments from these molecules were of lower masses, particularly, H^+, CH_n^+ ($n = 0$–6), $C_2H_n^+$, and $C_3H_n^+$, with C^+ dominating at all laser intensities. Though the yield of C^+ initially increases with laser intensity, due to the opening up of new channels for the formation of other cations, the relative yield of C^+ then decreases as seen in Figure 4. Figure 5 shows the power dependence of the ion yield for $C_2H_n^+$ and $C_3H_n^+$ fragments from anthracene. The relative yield of $C_3H_n^+$ is observed to decrease while the same for $C_2H_n^+$ ions increases indicating the decay of $C_3H_n^+$ to be a dominant process in the formation of $C_2H_n^+$.

Sequential loss of acetylene (C_2H_2) was identified as one of the major dissociation pathways in many earlier works on photodissociation of PAHs performed at laser intensities up to 10^{10} W cm^{-2} (Abakumov et al. 1981; Ekern et al. 1998; Poveda et al. 2009, 2012a). Present work at laser intensities of the order of 10^{13} W cm^{-2} gives no evidence for this channel. The presence of $C_{10}H_n^+$ formed by the loss of C_4H_n indicates that there is a pathway with loss of diacetylene. A minor peak around 50 amu reveals further ionization to form diacetylene, $C_4H_2^+$.

The power dependence of CH_4^+, CH_5^+, and CH_6^+ from the linear PAH molecules, anthracene and pentacene, are almost the same, as shown in Figure 6. Remarkably, the power dependence for the yield of fragments with less than three carbon atoms exhibits almost the same features for all three PAH molecules (Figure 7). This strongly suggests the same channels of formation for the lower masses from PAH molecules, irrespective of the number of aromatic rings in the parent molecule. The slopes of the curves for CH_n^+ ($n > 0$) from anthracene and pentacene were measured to be essentially the same (2.42) and are marked in Figure 3. However, the power dependence of CH_n^+ ($n = 4$–6) for phenanthrene is markedly different from that for anthracene and pentacene, indicating that the bent structure plays a role in determining the dissociation dynamics of these fragments.

Irrespective of the parent molecule, CH_4^+ shows the highest ascending rate with laser intensity among the carbon-containing fragment peaks. As discussed in the introduction, hydrocarbon ions with H/C ratio higher than one cannot be formed via direct photodissociation of PAH molecules. Thus the formation of these ions as observed in the present work involve complex processes that are intensified only at higher laser intensities and result in high ascending rates compared to other fragments in the spectra (see Figure 6). We propose a roaming mechanism preceded by intramolecular H-migrations to interplay in the formation of these ions. Scrambling and H-migration processes lead to large-scale chemical bond rearrangements. Wiersma et al. (2020) affirm that scrambling is common in PAH cations under UV radiation. Roaming dynamics involves the generation of a transient neutral atom, radical or molecule that "roams" around the remaining fragment and then abstracts a hydrogen atom from its counter fragment, before leaving the complex. CH_4 may partially cleave from a larger molecule formed after H-migration and can roam around the counter fragment, eventually leaving as CH_5^+ after proton abstraction. CH_4^+ may abstract H_2 to give CH_6^+. The newly formed CH_6^+ could detach a hydrogen atom to give CH_5^+. If a CH_5 neutral could form, then proton abstraction by CH_5 via the roaming mechanism can also lead to the formation of CH_6^+. Tsai et al. (2015) and Lin et al. (2018) report roaming signatures in the aliphatic aldehyde family and carbonyl compounds, respectively, and state that the roaming dissociation pathway becomes more predominant as the molecular size increases, as in the present work. Castellanos et al. (2018a, 2018b) invoke hydrogen roaming along the edges of the PAH molecules for the dehydrogenation pathways of photoinduced PAHs. To the best of our knowledge, roaming mechanisms in PAHs for the formation of fragment cations like CH_n^+ have not been studied for its dependence on the structure and size of PAHs, and the present results stress its importance.

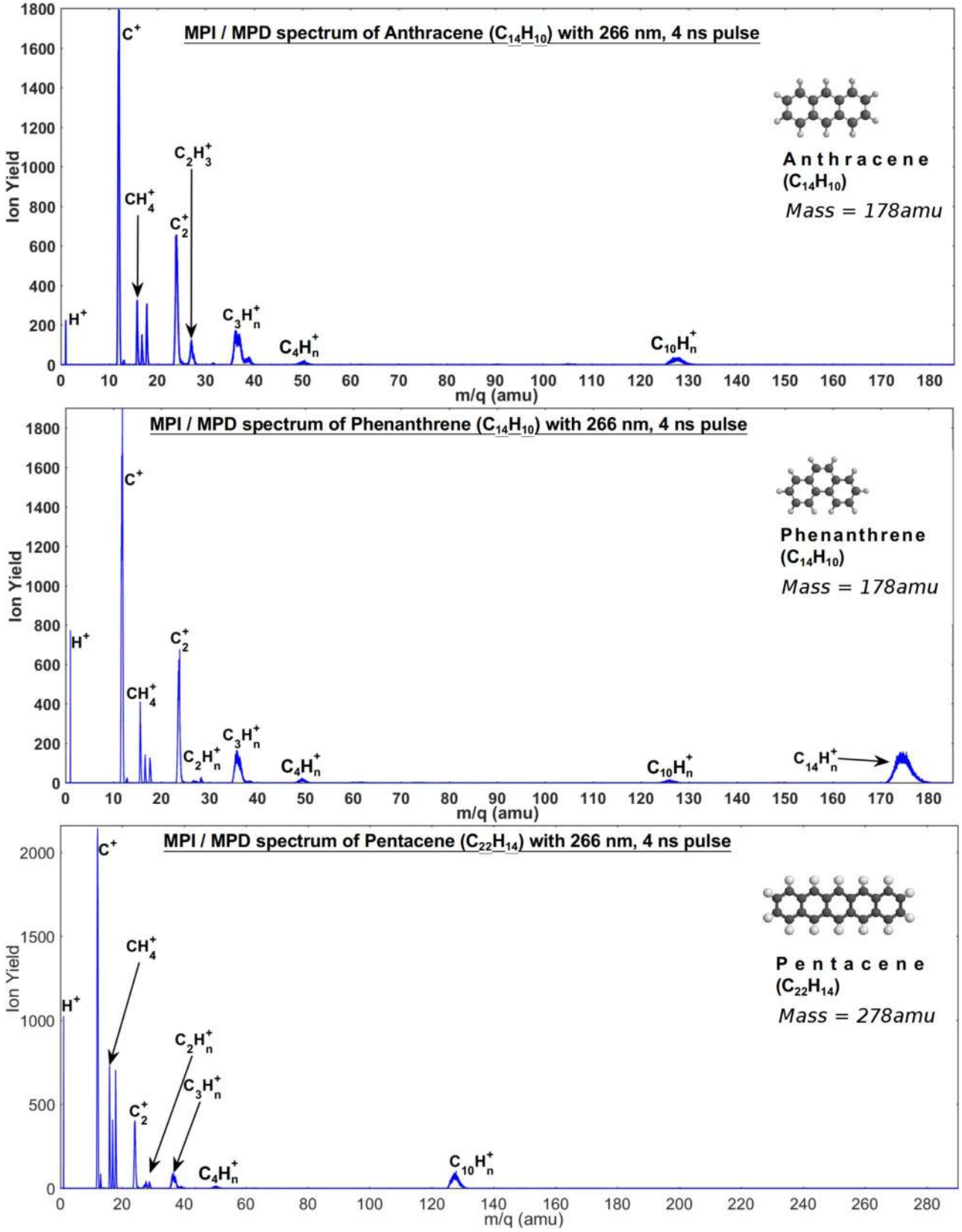

Figure 1. MPI/MPD spectra of anthracene, phenanthrene, and pentacene.

Fragment spectra of anthracene, phenanthrene, and pentacene, shown in Figure 2 reveal that the relative yield of CH_4^+, CH_5^+, and CH_6^+ are almost the same for the linear PAH molecules, anthracene and pentacene, but phenanthrene shows a different feature. In the case of phenanthrene, CH_4^+ peak is dominant compared to CH_5^+ and CH_6^+ while CH_6^+ is equally as

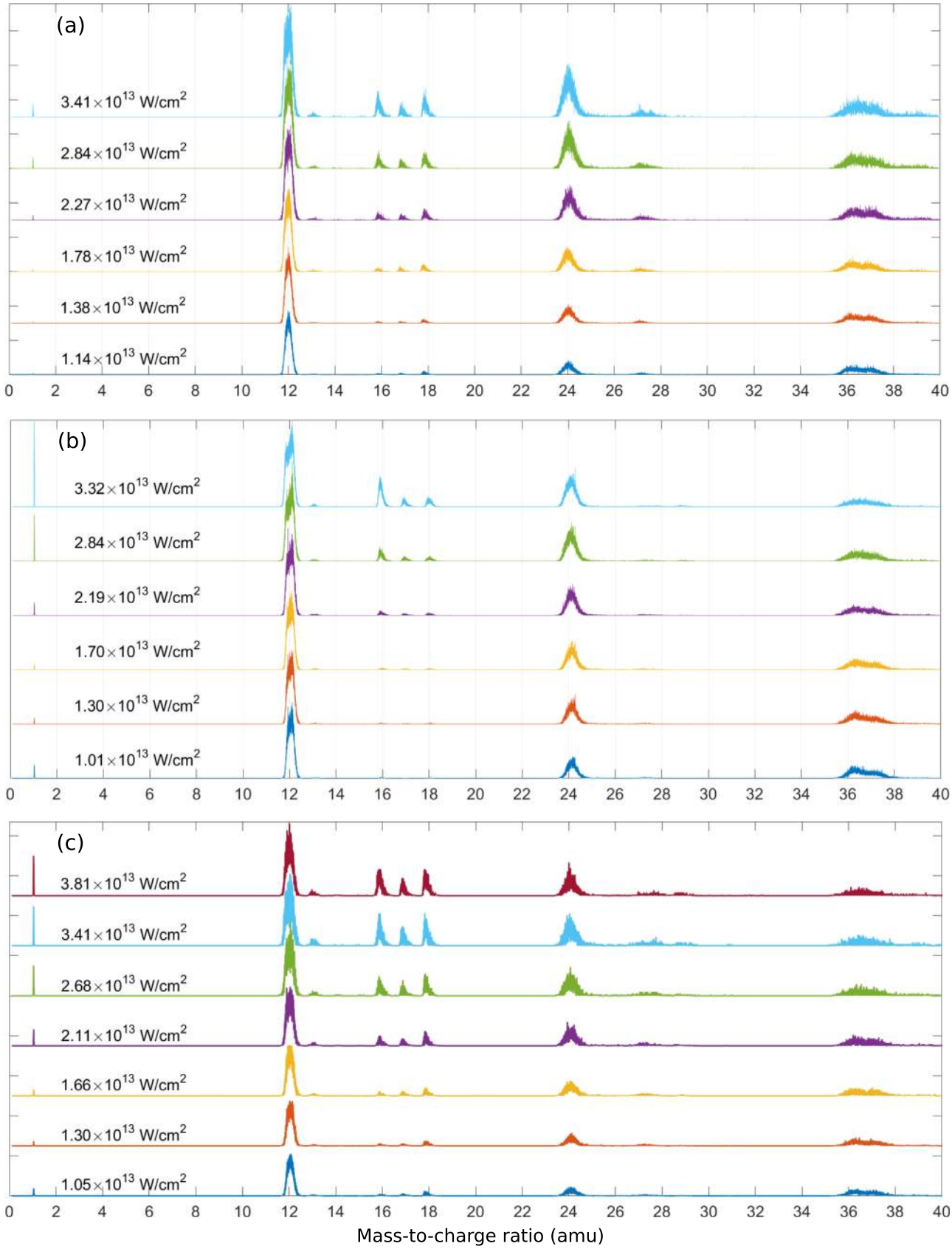

Figure 2. MPI/MPD spectra at different laser intensities for (a) anthracene, (b) phenanthrene, and (c) pentacene. Fragments of mass-to-charge ratio less than 40 amu are shown.

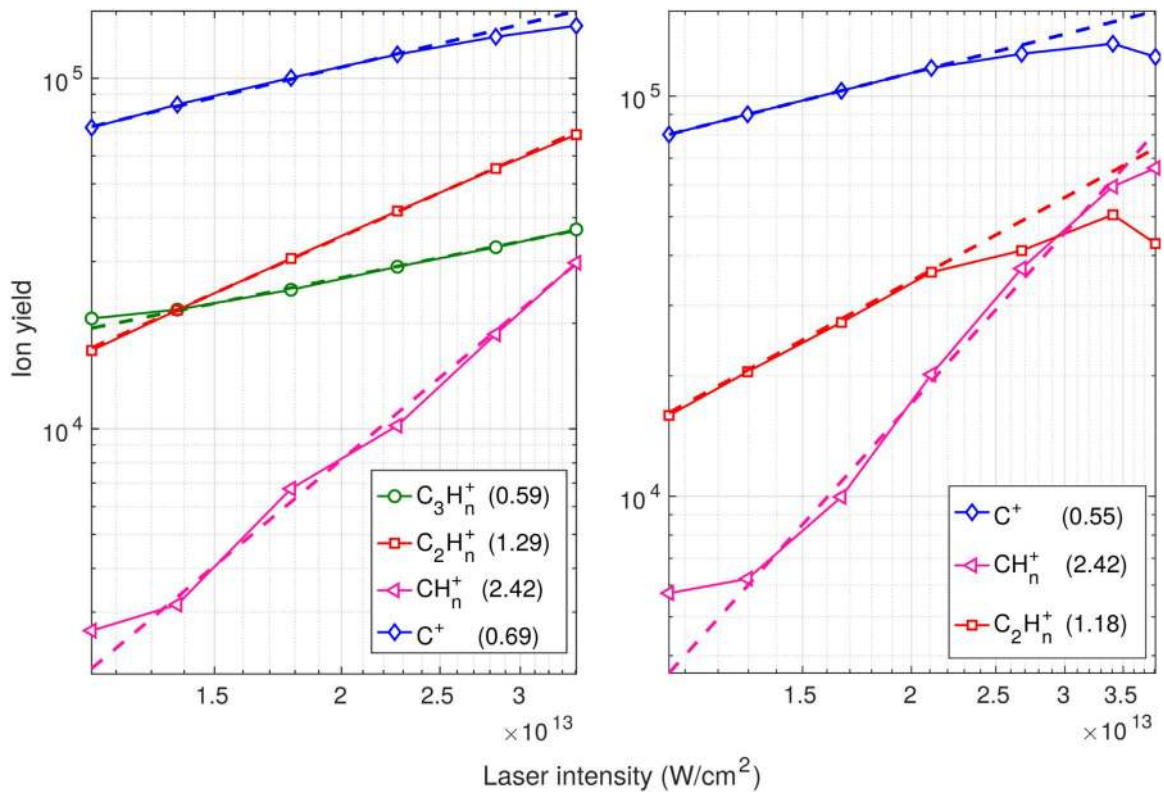

Figure 3. Power dependence of the yield of various fragments from anthracene (left) and pentacene (right). The slope of the fitted linear curve for each group is written in brackets.

strong as CH_4^+ in the anthracene and pentacene spectra. Table 1 compares the yield of CH_n^+ ($n = 4$–6) fragments from the three PAH parents upon photofragmentation. Phenanthrene gives lower yield compared to the linear benzenoids anthracene and pentacene except for CH_4^+ at higher laser powers. The bent structure of phenanthrene is observed to be weakening the roaming mechanism, when compared to its linear isomer, anthracene, yielding the observed result. The key molecular characteristic responsible for the roaming mechanism is the flat regions of the potential energy surface (PES) (Mauguière et al. 2017). The steric repulsion between the H-atoms in the bay region of the phenanthrene could shrink such regions (Grimme et al. 2009; Poater et al. 2018), thereby weakening the roaming mechanism. It is important to note that the formation of these three cations becomes more prominent with increasing laser intensities.

Our spectra also show the formation of $C_2H_3^+$ and $C_2H_5^+$, but the cross-sections are very low. These ions also cannot form by direct photodissociation from a PAH molecule. Their formation should be preceded by intramolecular hydrogen migration that leads to large-scale chemical bond rearrangements. The roaming mechanism could play a vital role in their formation.

3. Astrophysical Relevance

It is well understood that the photoionization and photodissociation processes critically determine the abundances of atomic and molecular species in diffuse interstellar clouds (Eddington 1928; Kramers & Ter Haar 1946; Bates & Spitzer 1951). The critical role of UV-photons in this regard has been briefly described in Heays et al. (2017), and the references therein provide a vast literature on these two processes. The photodissociation or photon-dominated regions (PDRs) are UV-rich regions in the space where the UV-radiation is 10^3–10^5 times more intense than the standard interstellar radiation field (Hollenbach & Tielens 1997). Photodissociation processes are of foremost importance in modeling the chemistry of almost every type of astrophysical region (Tielens & Hollenbach 1985; Sternberg & Dalgarno 1995; Glassgold 1996; Hollenbach & Tielens 1999; Le Petit et al. 2006; van Dishoeck et al. 2006; Glover & Clark 2012; Tielens 2013). In PDRs, the UV-photons are available for sufficient time aiding multiple excitations. In this perspective, a nanosecond pulse would be a more appropriate tool than a femtosecond pulse for studying the photofragmentations occurring in the ISM.

Small hydrocarbon chains (C_mH_n) are perceived to play active roles in the chemical networks that lead to the formation of many observed species in ISM (Prasad & Huntress 1980a, 1980b; Sternberg & Dalgarno 1995; Wakelam et al. 2012). Formation of CH_4^+, CH_5^+, and CH_6^+ observed in our spectra are of great astrophysical importance. CH_4^+ is a proposed ISM cation and CH_4 plays a major role in the hydrocarbon chemistry in dark clouds of ISM (Herzberg 1971; Gerlich 2005; Gerlich & Smith 2006). Protonated methane (CH_5^+) is a remarkably exceptional molecule that is suspected to be found in the ISM (Herzberg 1971; Gerlich & Horning 1992; Gerlich 2005; Mann et al. 2008; Gerlich & Borodi 2009). These molecules play vital roles in the deuterium fractionation in the ISM, thus controlling the D/H ratio (Asvany et al. 2004a, 2004b; Schlemmer et al. 2005; Parise et al. 2009; Roueff et al. 2013; Treviño-Morales et al. 2014).

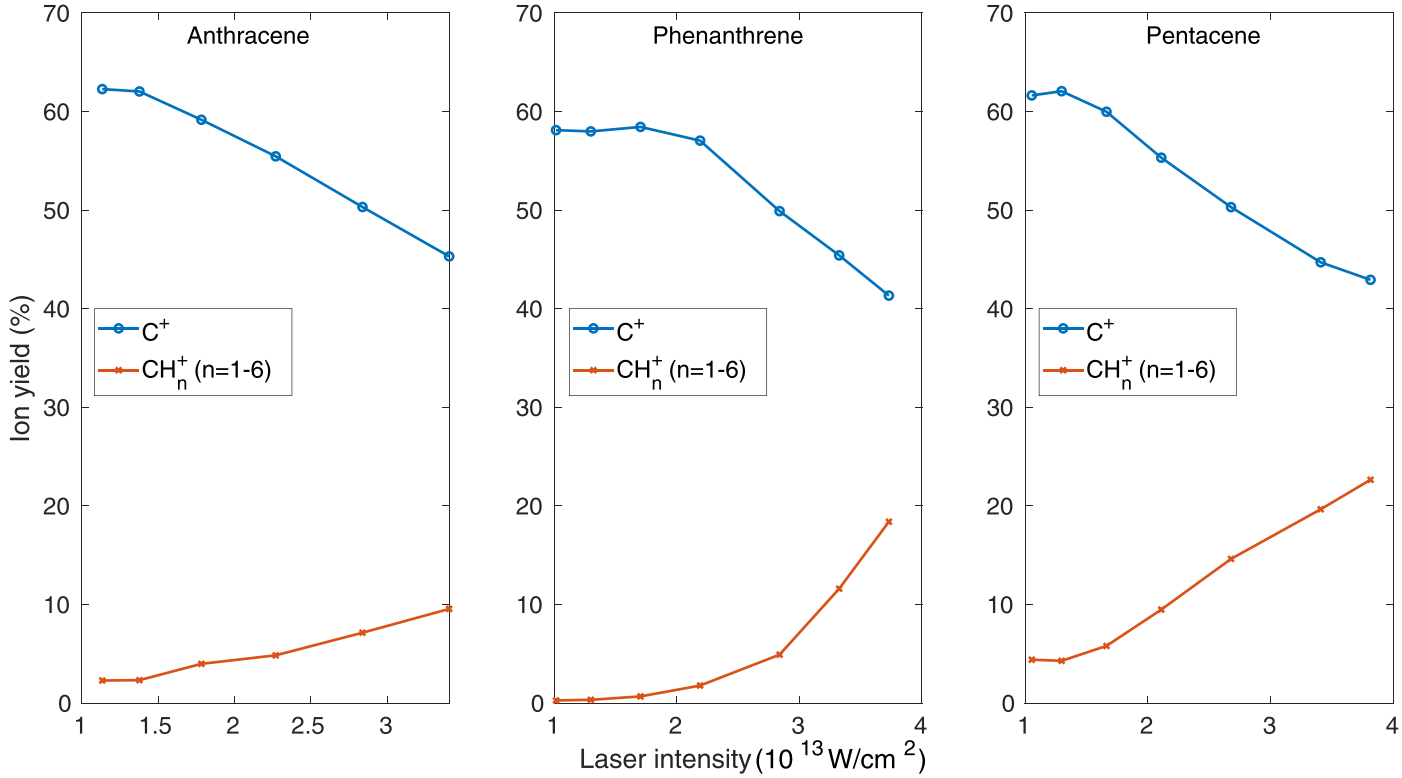

Figure 4. Percentage of fragment ion yield is plotted against the laser intensity. The % yield of C^+ goes down with laser intensities as a result of the enhanced formation of new fragment ions at higher laser intensities. The contribution of CH_n^+ (n = 1–6) with laser intensity exhibits an enhancement with increasing laser intensity. This is the case for most of the other fragment ions too.

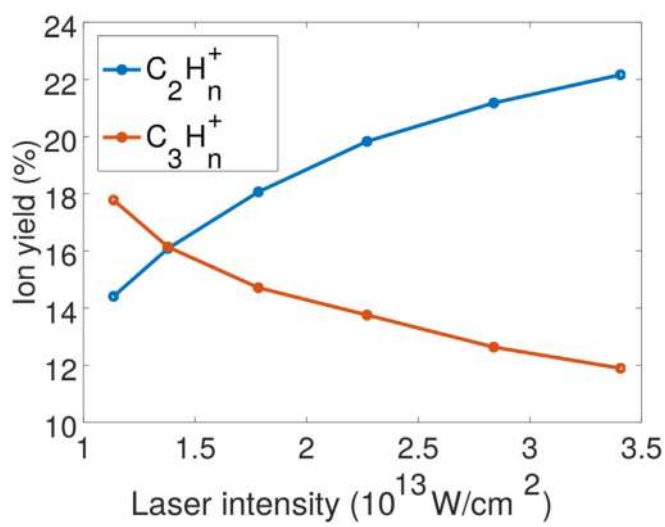

Figure 5. Percentage of ion yield of $C_2H_n^+$ and $C_3H_n^+$ in total ion yield is plotted against the laser intensity.

One of the abundant ISM molecules, CH_4 is thought to be formed mainly by hydrogenation of carbon atoms on the grain surfaces (Hiraoka et al. 1998; Qasim et al. 2020). In the gas phase, the potential pathway of the formation of CH_4 is proposed to include CH_5^+, for example, $CH_5^+ + CO \rightarrow CH_4 + HCO^+$. Repeated reactions of carbon with H_2 with CH_5^+ as an intermediate is also considered to yield CH_4 (Rehder 2010). The electronic recombination of CH_5^+ is considered as another likely way in the gas-phase to form CH_4 (Kokoouline et al. 2011). This pathway is also considered for other simple molecules (Garrod & Herbst 2006). CH_5^+ could also undergo reactions leading to the formation of simple molecules in the ISM such as $(CH_3)_2O$, C_6H_6, and CH_3OH. A rigorous search is ongoing to assign rotational and vibrational spectra of CH_5^+ via novel experimental methods since the constantly moving five hydrogen atoms make it challenging to probe via conventional methods (White et al. 1999; Asvany et al. 2005; Huang et al. 2006; Wang & Carrington 2016). CH_5^+ and CH_6^+ cannot form in ISM from their neutral counterparts. It must be forming either from lower molecules through several reactions or by photodissociation of larger molecules such as PAHs. H-migration and the roaming mechanism are expected to be strong in large molecules such as the PAHs. Formation of CH_n^+ (n = 4–6) from a larger precursor upon photodissociation is not probed, and our present results urge the need to search these ions in the UV-rich PDRs, where photodissociation of PAHs could occur, as observed in the present work. Roaming mechanism is a possible mediation in interstellar chemistry concerning the single carbon hydrocarbons as well as H (D), H_2 (D_2), and their cations. The roaming mechanism has been recently suggested for ISM chemistry of lower mass molecules under strong-field photodissociation (Ekanayake et al. 2018a, 2018b). We propose its potential role in even larger hydrocarbon molecules in the ISM. The ISM, being a low-density environment, should facilitate this mechanism. Our results show that the cross-section for the formation of CH_n^+ (n = 4–6) from linear PAH molecules is more favorable compared to the bent structured PAHs, as flat regions in the PESs enhance the roaming mechanism. As mentioned earlier, the kinked PAHs have bay regions with H-atoms, thus suffering steric repulsion, which can shrink the flat regions in the PES. This

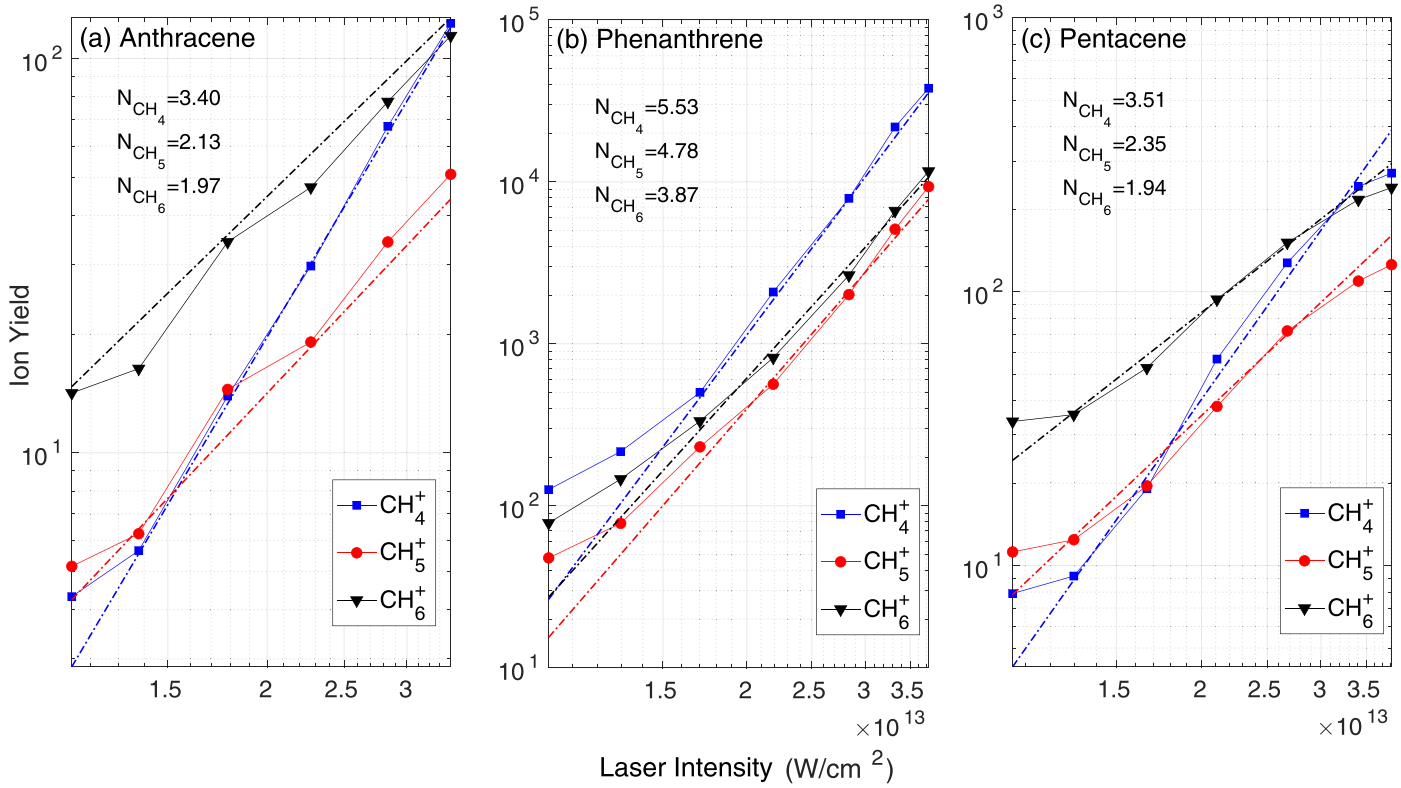

Figure 6. Ion yield vs. laser intensity for CH_4^+, CH_5^+, and CH_6^+. Dotted lines are linear fit to the linearly varying portions of the curves in log–log plots. Slopes of the fitted curves, identified as the number of photons involved in the process of formation, are written as N in the insets.

Table 1
Ratio of the Yield of CH_n^+ (n = 4–6) Fragments from Anthracene, Phenanthrene, and Pentacene at Three Different Laser Powers, Respectively

Laser Power (mW)	CH_4^+	CH_5^+	CH_6^+
~165	0.62:0.24:1	0.50:0.06:1	0.46:0.04:1
~210	0.73:0.26:1	0.74:0.12:1	0.65:0.06:1
~410	0.51:0.90:1	0.46:0.46:1	0.53:0.31:1

leads to the observed (Figure 2) relatively lower yield of CH_n^+ (n = 4–6) from the phenanthrene parent than anthracene and pentacene under a strong laser field.

Our results on the anthracene–phenanthrene isomer pairs reveals higher survivability of the phenanthrene cation against photodissociation compared to anthracene. This indicates higher photostability of nonlinear PAHs in the ISM compared to their linear isomers, and that nonlinear PAHs could be a more prominent source of these fluxional ions. Studies by Sabirov et al. (2018) associate minimum polarizability for higher abundance among isomeric interstellar compounds. Our results are in agreement with this as phenanthrene has lower mean polarizability than anthracene. Thus we can expect higher stability of nonlinear PAHs in the ISM compared to their linear isomers against UV irradiations in ISM. On the other hand, pentacene, which has higher mean polarizability than anthracene and phenanthrene, shows a greater degree of fragmentation compared to the other two.

The abundance of C_3H_2 in the UV-rich regions remains unexplained (Gerin et al. 2003; Savić & Gerlich 2005; Savić et al. 2005). c–C_3H_2 is widely distributed in the ISM (Matthews & Irvine 1985; Matthews et al. 1986; Cox et al. 1988; Lucas & Liszt 2000). The proposed modes of formation for C_3H_2 in ISM are radiative association of C_3H^+ with H_2 and hydrogen abstraction of C_3H^+ (Gerlich & Horning 1992). c–C_3H_2 has been recently detected abundantly toward some selected PDRs of ISM and it was suggested that the photoerosion of UV-irradiated PAHs could be efficiently feeding the ISM with small hydrocarbons like c–C_3H_2 (Fossé et al. 2000; Fuente et al. 2003; Teyssier et al. 2004; Pety et al. 2005; Guzmán et al. 2015). Multiphoton ionization/multiphoton dissociation (MPI/MPD) spectra of the PAH molecules in the current study show the formation of the C_3 H_2^+ cation. Thus our experimental results imply that the UV-photodestruction of PAH molecules could be a vital source for C_3H_2 in such regions. Our results also show a possible decay of three carbon hydrocarbons to two carbon hydrocarbons under strong-field conditions.

Sequential loss of acetylene (C_2H_2) is generally understood as a prominent decay pathway of PAH molecules in ISM (Gotkis et al. 1993; Poveda et al. 2010, 2012b; West et al. 2012; Najeeb & Kadhane 2017). Absence of sequential loss of C_2H_2 at high laser intensities in the present photodissociation spectra implies that this decay pathway is unlikely to be triggered by UV-photons in the UV-rich regions of the ISM. Similarly, the absence of CH^+ as a fragment in our experiment shows that UV-photodissociation of PAHs may not play a role in the formation of this abundant ISM cation (Dunham 1937; Douglas & Herzberg 1941; Indriolo et al. 2010).

High laser intensities in our experiments lead to multiphoton absorption by PAHs. Although in the ISM, such light intensities are absent, single-photon absorption in the broadband UV environment would lead to ionization, and the excited

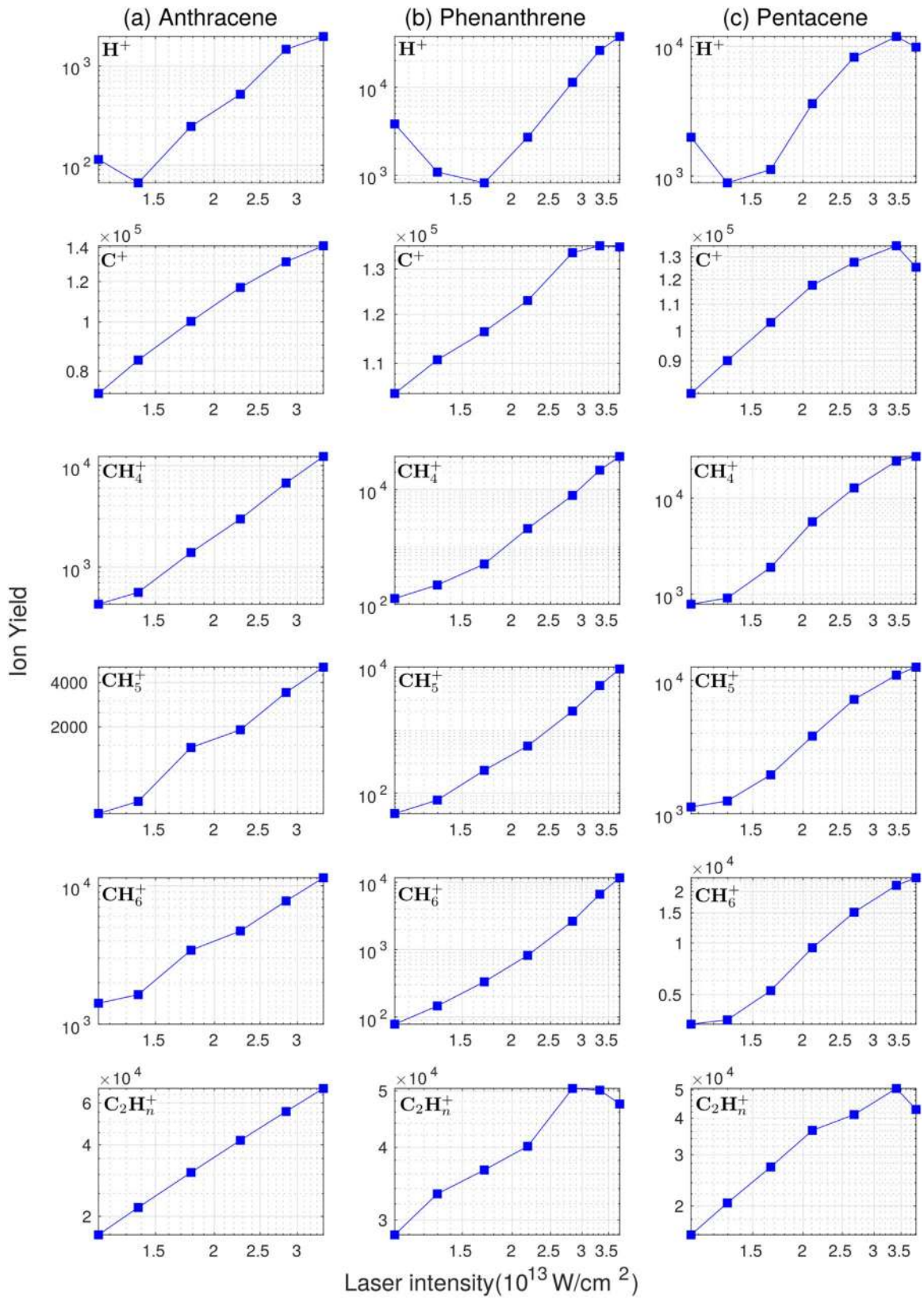

Figure 7. Laser power dependence for the yield of fragments with fewer than three carbon atoms.

cation would undergo the same fragmentation processes via intramolecular vibrational relaxation. Any fragmentation that occurs sequentially in our experiment would also occur in the ISM due to the constant broadband UV. However, we should expect differences in the yields of the fragments arising from the differences in the cross-sections for multiphoton and single-photon processes, the latter being higher, we expect higher yields of the observed fragments in the ISM. Generally, PAHs

resonantly absorb light around 220 nm, which rules out resonant-multiphoton absorption in the present case. The roaming mechanism and the hydrogen abstraction play the same role in the multiphoton and the ISM UV conditions. We believe that the present results motivate further probes of PAHs cations as a source of CH_n^+ ($n = 4$–6) ions in the ISM and theoretical and experimental investigations on the proposed roaming mechanisms.

This work was supported by the Board of Research in Nuclear Sciences (BRNS) under the project 2012/37P/45/BRNS.

ORCID iDs

Roby Chacko https://orcid.org/0000-0002-0792-7736

References

Abakumov, G. A., Anisimov, Y. M., Kupriyanov, S. E., et al. 1981, QuEle, 11, 268
Allamandola, L. J., Tielens, A. G. G. M., & Barker, J. R. 1987, in Physical Processes in Interstellar Clouds, ed. G. Morfill & M. Scholer (Springer: Dordrecht), 305
Antonov, V. S., & Letokhov, V. S. 1981, ApPhy, 24, 89
Asvany, O., Padma Kumar, P., Redlich, B., et al. 2005, Sci, 309, 1219
Asvany, O., Savić, I., Schlemmer, S., & Gerlich, D. 2004a, CP, 298, 97
Asvany, O., Schlemmer, S., & Gerlich, D. 2004b, ApJ, 617, 685
Balsiger, H., Altwegg, K., Buhler, F., et al. 1987, A&A, 187, 163
Bates, D. R., & Spitzer, L. J. 1951, ApJ, 113, 441
Bowman, J. M., & Houston, P. L. 2017, Chem. Soc. Rev., 46, 7615
Bowman, J. M., & Suits, A. G. 2011, PhT, 64, 33
Castellanos, P., Candian, A., Andrews, H., & Tielens, A. G. G. M. 2018a, A&A, 616, A167
Castellanos, P., Candian, A., Zhen, J., Linnartz, H., & Tielens, A. G. G. M. 2018b, A&A, 616, A166
Cernicharo, J., Liu, X.-W., González-Alfonso, E., et al. 1997, ApJL, 483, L65
Cox, P., Guesten, R., & Henkel, C. 1988, A&A, 206, 108
Douglas, A. E., & Herzberg, G. 1941, ApJ, 94, 381
Dunham, T. 1937, PASP, 49, 26
Eddington, A. S. 1928, MNRAS, 88, 352
Ekanayake, N., Nairat, M., Weingartz, N. P., et al. 2018a, JChPh, 149, 244310
Ekanayake, N., Severt, T., Nairat, M., et al. 2018b, NatCo, 9, 5186
Ekern, S. P., Marshall, A. G., Szczepanski, J., & Vala, M. 1998, JPCA, 102, 3498
Fossé, D., Cesarsky, D., Gerin, M., Lequeux, J., & Tiné, S. 2000, EPASP, 456, 91
Fuente, A., Rodriguez-Franco, A., Garcia-Burillo, S., Martin-Pintado, J., & Black, J. H. 2003, A&A, 406, 899
Garrod, R. T., & Herbst, E. 2006, A&A, 457, 927
Gerin, M., Fossé, D., & Roueff, E. 2003, in Chemistry as a Diagnostic of Star Formation, ed. C. L. Curry & M. Fich (Ottawa: NRC Research Press), 81
Gerlich, D. 2005, PCCP, 7, 1583
Gerlich, D., & Borodi, G. 2009, FaDi, 142, 57
Gerlich, D., & Horning, S. 1992, ChRv, 92, 1509
Gerlich, D., & Smith, M. 2006, PhyS, 73, C25
Glassgold, A. E. 1996, ARA&A, 34, 241
Glover, S. C. O., & Clark, P. C. 2012, MNRAS, 421, 116
Gotkis, Y., Oleinikova, M., Naor, M., & Lifshitz, C. 1993, JPCA, 97, 12282
Grimme, S., Mück-Lichtenfeld, C., Erker, G., et al. 2009, Angew. Chemie Int. Ed., 48, 2592
Guzmán, V. V., Pety, J., Goicoechea, J. R., et al. 2015, ApJL, 800, L33
Heays, A. N., Bosman, A. D., & van Dishoeck, E. F. 2017, A&A, 602, A105
Herzberg, G. 1971, Q. Rev., Chem. Soc., 25, 201
Hiraoka, K., Miyagoshi, T., Takayama, T., Yamamoto, K., & Kihara, Y. 1998, ApJ, 498, 710
Hollenbach, D. J., & Tielens, A. G. G. M. 1997, ARA&A, 35, 179
Hollenbach, D. J., & Tielens, A. G. G. M. 1999, RvMP, 71, 173
Huang, X., McCoy, A. B., Bowman, J. M., et al. 2006, Sci, 311, 60
Indriolo, N., Oka, T., Geballe, T. R., & McCall, B. J. 2010, ApJ, 711, 1338
Iwamoto, N., Schwartz, C. J., Jochim, B., et al. 2020, JChPh, 152, 054302
Kling, N. G., Díaz-Tendero, S., Obaid, R., et al. 2019, NatCo, 10, 1
Kokoouline, V., Douguet, N., & Greene, C. H. 2011, CPL, 507, 1
Kramers, H. A., & Ter Haar, D. 1946, BAN, 10, 137
Le Petit, F., Nehme, C., Le Bourlot, J., & Roueff, E. 2006, ApJS, 164, 506
Lin, K.-C., Tsai, P.-Y., Chao, M.-H., et al. 2018, IRPC, 37, 217
Lucas, R., & Liszt, H. S. 2000, A&A, 358, 1069
Mann, J. E., Xie, Z., Savee, J. D., et al. 2008, JAChS, 130, 3730
Marciniak, A., Despré, V., Barillot, T., et al. 2015, NatCo, 6, 7909
Matthews, H. E., Avery, L. W., Madden, S. C., & Irvine, W. M. 1986, ApJL, 307, L69
Matthews, H. E., & Irvine, W. M. 1985, ApJL, 298, L61
Mauguière, F. A., Collins, P., Kramer, Z. C., et al. 2017, ARPC, 68, 499
McCoy, A. B., Braams, B. J., Brown, A., et al. 2004, JPCA, 108, 4991
Mineo, H., Chao, S. D., Kato, T., & Yamanouchi, K. 2013, J. Chin. Chem. Soc., 60, 1207
Najeeb, P. K., & Kadhane, U. 2017, IJMSp, 414, 23
Parise, B., Leurini, S., Schilke, P., et al. 2009, A&A, 508, 737
Peeters, E. 2011, in IAU Symp. 280, The Molecular Universe (Cambridge: Cambridge Univ. Press), 149
Pety, J., Teyssier, D., Fossé, D., et al. 2005, A&A, 435, 885
Poater, J., Duran, M., & Solà, M. 2018, FrCh, 6, 561
Poveda, J., Álvarez, I., & Cisneros, C. 2012a, J. Photochem. Photobiol. A, 230, 31
Poveda, J., Álvarez, I., & Cisneros, C. 2013, MolPh, 111, 19
Poveda, J., Guerrero, A., Álvarez, I., & Cisneros, C. 2010, J. Photochem. Photobiol. A, 215, 140
Poveda, J., San Román, A., Guerrero, A., Álvarez, I., & Cisneros, C. 2008, Int. J. Mol. Sci., 9, 2003
Poveda, J. C., Álvarez, I., & Cisneros, C. 2012b, in Naphthalene: Structure, Properties and Applications, ed. G. I. Antsyforov & A. F. Ivanski (1st ed.; Hauppauge, NY: Nova Science Publishers), 59
Poveda, J. C., Guerrero, A., Álvarez, I., & Cisneros, C. 2009, RMxF, 55, 312
Prasad, S. S., & Huntress, W. T. J. 1980a, ApJS, 43, 1
Prasad, S. S., & Huntress, W. T. J. 1980b, ApJ, 239, 151
Qasim, D., Fedoseev, G., Chuang, K.-J., et al. 2020, NatAs, in press
Rehder, D. 2010, Chemistry in Space (Weinheim: Wiley-VCH), 45
Robson, L., Tasker, A., Ledingham, K., et al. 2002, IJMSp, 220, 69
Roueff, E., Gerin, M., Lis, D. C., et al. 2013, JPCA, 117, 9959
Sabirov, D. S., Garipova, R. R., & Cataldo, F. 2018, MolAs, 12, 10
Salama, F., Bakes, E. L. O., Allamandola, L. J., & Tielens, A. G. G. M. 1996, ApJ, 458, 621
Salama, F., Galazutdinov, G. A., Krełowski, J., Allamandola, L. J., & Musaev, F. A. 1999, ApJ, 526, 265
Savić, I., & Gerlich, D. 2005, PCCP, 7, 1026
Savić, I., Schlemmer, S., & Gerlich, D. 2005, ApJ, 621, 1163
Schlemmer, S., Asvany, O., Hugo, E., & Gerlich, D. 2005, in IAU Symp. 231, Astrochemistry: Recent Successes and Current Challenges, ed. D. C. Lis, G. A. Blake, & E. Herbst (Cambridge: Cambridge Univ. Press), 125
Sternberg, A., & Dalgarno, A. 1995, ApJS, 99, 565
Suits, A. G. 2008, Acc. Chem. Res., 41, 873
Teyssier, D., Fossé, D., Gerin, M., et al. 2004, A&A, 417, 135
Tielens, A. G. G. M. 2013, RvMP, 85, 1021
Tielens, A. G. G. M., & Hollenbach, D. 1985, ApJ, 291, 747
Townsend, D., Lahankar, S. A., Lee, S. K., et al. 2004, Sci, 306, 1158
Treviño-Morales, S. P., Pilleri, P., Fuente, A., et al. 2014, A&A, 569, A19
Tsai, P.-Y., Li, H.-K., Kasai, T., & Lin, K.-C. 2015, PCCP, 17, 23112
van Dishoeck, E. F., Jonkheid, B., & van Hemert, M. C. 2006, FaDi, 133, 231
Wakelam, V., Herbst, E., Loison, J.-C., et al. 2012, ApJS, 199, 21
Wang, X.-G., & Carrington, T., Jr. 2016, JChPh, 144, 204304
West, B., Joblin, C., Blanchet, V., et al. 2012, JPCA, 116, 10999
White, E. T., Tang, J., & Oka, T. 1999, Sci, 284, 135
Wiersma, S. D., Candian, A., Bakker, J. M., et al. 2020, A&A, 635, A9
Wiley, W. C., & McLaren, I. H. 1955, RScI, 26, 1150
Wörner, H. J., Qian, X., & Merkt, F. 2007, JChPh, 126, 144305
Wu, H., Xue, Y., Wen, J., et al. 2019, RSC Adv., 9, 16683